

Square and bow-tie configurations in the cyclic evasion problem

M.D. Arnold, M. Golich, A. Grim, L. Vargas, V. Zharnitsky

MA: University of Texas at Dallas, Richardson, TX, USA

MG: Purdue University, West Lafayette, IN, USA

AG: University of St. Thomas, St Paul, MN, USA

LV: Instituto Tecnológico Autónomo de México, Mexico City, Mexico

VZ: University of Illinois at Urbana-Champaign, Urbana, IL, USA

E-mail: vzh@illinois.edu

Abstract. Cyclic evasion of four agents on the plane is considered. There are two stationary shapes of configurations: square and degenerate bow-tie. The bow-tie is asymptotically attracting while the square is of focus-center type. Normal form analysis shows that square is nonlinearly unstable. The stable manifold consists of parallelograms that all converge to the square configuration. Based on these observations and numerical simulations, it is conjectured that any non-parallelogram non-degenerate configuration converges to the bow-tie.

Keywords: Cyclic evasion, stability, Lyapunov function, normal forms.

Submitted to: *Nonlinearity*

1. Introduction.

The study of pursuit and evasion has a long rich history in mathematics. In the past several decades, there has been revival of interest to these problems because of the connection with the field of decentralized control. In control applications, the following systems often arise: for a given ordered set of n agents $\mathbf{a}_1, \mathbf{a}_2, \dots, \mathbf{a}_n$ one associates the *connectivity* matrix A . The velocity of the j -th agent is then given by some function of its relative position $z_j - z_i$ to those agents \mathbf{a}_i for which $A_{i,j} \neq 0$.

One of the basic examples of such models is given by the cyclic pursuit problem where matrix A is a circulant matrix of the cyclic index-shift. Such systems were studied by several authors, see *e.g.* [6], [8], [12], [13] and references therein, with the main goal to provide conditions on the controllable rendezvous, *i.e.* when the agents converge to the same point on the plane.

In the simplest case of the cyclic pursuit model, each agent moves with the unit speed toward the forerunner. Such model can be thought of as a variant of discretization

of a curve-shortening flow. For planar systems, this analogy is also reflected in the limiting behavior of the configurations: both converge to a point and in the limit the shape of almost every configuration tends to the regular polygon. We refer the reader to an interesting book [11] for the review of the results in this direction. There are also generalizations of curve shortening and cyclic pursuit to other manifolds, see [9].

From the applications viewpoint, it is natural to introduce some bearing angle in the cyclic pursuit, *i.e.* to make the velocity of the j -th agent to have some constant angle ϕ with the direction to the $j - 1$ -st agent, see [1], [8], [13]). In [13] it was shown that if the angle ϕ is not too large, almost any configuration converges to a point. This can be thought of as a strong contraction of the curve shortening. In [1] a local analysis of the stable configurations for arbitrary bearing angles was done.

There is an interesting example of configuration dependent bearing angle when each agent moves in the direction normal to the bisector of the corresponding angle. Such flow is useful in the theory of billiards [5].

In the present paper we consider the particular case $\phi = \pi$ which we will call *cyclic evasion*. The cyclic evasion can be thought of as a discrete version of a curve lengthening flow.

This problem was studied in theoretical computer science literature, see [2] and references therein, and one of the basic conclusions was that a generic initial configuration converges to a invariant configuration that has the largest perimeter growth. In [2] this observation was verified for the simplest case of 3 agents. It was found that if the initial configuration is a non-degenerate triangle then the limiting shape is an equilateral triangle. This was achieved by constructing a global Lyapunov function.

From the results in [1], it follows that if $n > 4$, then regular convex n -gons are linearly unstable shapes in the cyclic evasion problem. Since for sufficiently large n there are several linearly stable shapes no obvious candidate for a global Lyapunov function can be expected.

A linear analysis of appropriately reduced system shows that there are only two constant angle configurations in the system for $n = 4$: square and line configurations. The line configurations are of two types: cyclic and bow-tie configuration. It turns out that bow-tie is linearly stable and attracting, while the family of cyclic line configurations is unstable. The square configuration is neutrally stable in linear approximation and further analysis of the normal form shows that the square is nonlinearly unstable.

Structure of the paper

In the next section we introduce an appropriately reduced system in the shape-space that takes into account all symmetries in the problem. We derive the main equations governing cyclic evasion dynamics. In section 3 we describe the stable points for the cyclic evasion dynamics in the shape-space and perform linear analysis near these points. In section 4 we observe that the space of parallelograms is an invariant subspace. We derive the equations for the reduced system in this space and prove the global stability

of the square configuration for the reduced dynamics. Section 5 is devoted to the non-linear analysis of the square configuration in the whole 4-dimensional shape-space. In the last section we present a discussion of our results. We also provide an appendix with Mathematica notebook which was used to compute the Lyapunov number that is relevant for nonlinear stability.

Acknowledgments

Major part of this research was carried out during the Summer@ICERM 2015 program at ICERM, Brown University. The authors are grateful to the ICERM for hospitality and creating a stimulating research environment. Authors also appreciate lengthy, deep and fruitful discussions with S. Tabachnikov, Yu. Baryshnikov, and S. Klajbor-Goderich. VZ was partially supported by a grant from the Simons Foundation # 278840.

2. Shapes of configurations.

In this article, all indices are defined modulo 4. The equations of cyclic evasion for 4 agents are given by the following system of equations, see Figure 1:

$$\dot{z}_j = \frac{z_j - z_{j-1}}{|z_j - z_{j-1}|}, \quad j = 1, \dots, 4, \quad (1)$$

where $z_j(t) \in \mathbb{C}$ is the coordinate of the j -th agent \mathbf{a}_j written as a complex number. We will consider only those configurations where dynamics is well defined, *i.e.* we exclude configurations $\Lambda = \{(z_1, z_2, z_2, z_4), z_{i+1} = z_i, \text{ for some } i\}$. We will be mostly interested in

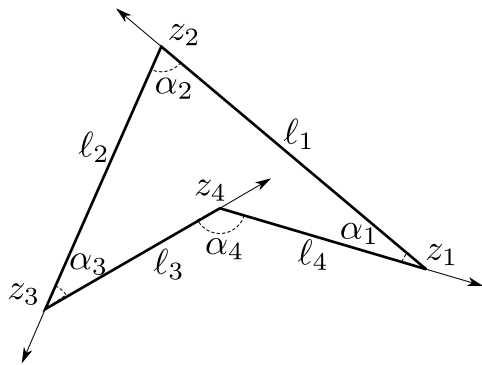


Figure 1. Cyclic Evasion.

the shape of the polygonal chain $\{z_1, z_2, z_3, z_4\}$, *i.e.* we will identify two configurations differing by a translation, rotation and scaling. While the configuration space for the system (1) consists of all quadruples z_j , we can always shift the origin to the position of the first agent and choose the coordinate system in such a way that the position of second agent will have coordinates $1 + 0i$. This change of coordinates correspond to the translation by vector $-z_1$ and then to the scaling by the vector $z_2 - z_1$. Thus, the space of shapes of the configurations which we will be interested in is homeomorphic to a subset of $\mathbb{C}^3 / \sim_{\mathbb{C}} = \mathbb{C}\mathbb{P}^2$ where singular points corresponding to Λ are removed.

To describe the dynamics, it is natural to choose as local coordinates side-lengths l_j and angles α_j , see [1]. The system of 8 ODEs is then given by

$$\begin{cases} \dot{l}_j = 1 + \cos(\alpha_{j-1}) \\ \dot{\alpha}_j = \frac{\sin(\alpha_{j-1})}{l_j} - \frac{\sin(\alpha_j)}{l_{j+1}} \end{cases} \quad (2)$$

From these equations, it follows that stationary shapes of the cyclic evasion correspond to the formations whose side lengths grow at the same speed. That is \dot{l}_j and correspondingly $\cos(\alpha_j)$ do not depend on j . Therefore, for any i and j one has either $\alpha_j = \alpha_i$ or $\alpha_j = \pi - \alpha_i$. Together with the closing condition $\alpha_1 + \alpha_2 + \alpha_3 + \alpha_4 = 2\pi$ this leaves us only three possibilities:

- $\alpha_1 = \alpha_2 = \alpha_3 = \alpha_4 = \pi/2$. In such a case from the second equation of the system (2) we obtain the condition $0 = \dot{\alpha}_j = \frac{1}{l_j} - \frac{1}{l_{j+1}}$ which yields $l_j = l_{j+1}$. Thus, one of the stationary configurations correspond to the square formation.
- $\alpha_1 = \alpha_3 = \pi, \alpha_2 = \alpha_4 = 0$. Bow-tie configuration.
- $\alpha_1 = \alpha_2 = \pi, \alpha_3 = \alpha_4 = 0$. Cyclic degenerate configuration.

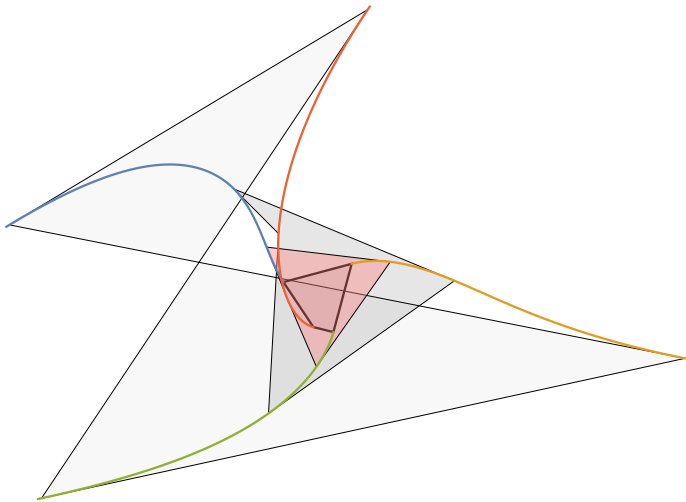


Figure 2. Simulation of the four-bug evasion leading to the loss of convexity.

We finish this section with a simple statement about convexity.

Proposition 1. *The set of non-convex configurations is forward invariant.*

In other words, if during the evolution the convexity is lost, then it cannot be restored. Indeed, consider the border line case, when one of the agents is on the line between the other two, e.g. z_2 is on the line connecting z_3 and z_4 , see Figure 1. At the next instant $t + dt$ the configuration will become non-convex, as z_1, z_4 will stay on the same line with the accuracy $O(dt^2)$ while z_3 will move by $O(dt)$ in non-convex direction.

3. Linear Stability.

In order to perform linear stability analysis we rewrite system (1) in the new variables using translation, rotation, and scaling symmetries.

We define a local frame in such a way that the first bug is always located at the origin and the coordinate of the second bug is $1 + 0i$. As we stated earlier, our original configuration space contains only nondegenerate configurations: $\{z_1, z_2, z_3, z_4 \in \mathbb{C}^4, z_i \neq z_j \text{ if } |i - j| = 1\}$.

We will translate our dynamical system (1) to the new coordinates by transform

$$w = \frac{z - z_1}{z_2 - z_1},$$

but it will be more convenient to do this in two steps that are described next.

Our first transformation is given by

$$v = z - z_1,$$

so the new equations become

$$\dot{v}_j = \dot{z}_j - \dot{z}_1 = \frac{z_j - z_{j-1}}{|z_j - z_{j-1}|} - \frac{z_1 - z_4}{|z_1 - z_4|} = \frac{v_j - v_{j-1}}{|v_j - v_{j-1}|} - \frac{v_1 - v_4}{|v_1 - v_4|},$$

where $j = 2, 3, 4$ and $v_1 = 0$. The second transformation is given by rescaling:

$$w = v/v_2,$$

so that we have for $j = 3, 4$

$$\dot{w}_j = \frac{1}{v_2} \left(\frac{v_j - v_{j-1}}{|v_j - v_{j-1}|} - \frac{v_1 - v_4}{|v_1 - v_4|} \right) - \frac{v_j}{v_2^2} \left(\frac{v_2 - v_1}{|v_2 - v_1|} - \frac{v_1 - v_4}{|v_1 - v_4|} \right).$$

Dividing by v_2 , we obtain the reduced system in w variables:

$$\dot{w}_j = \frac{1}{v_2} \left(\frac{w_j - w_{j-1}}{|w_j - w_{j-1}|} - \frac{w_1 - w_4}{|w_1 - w_4|} \right) - \frac{w_j}{v_2} \left(\frac{w_2 - w_1}{|w_2 - w_1|} - \frac{w_1 - w_4}{|w_1 - w_4|} \right),$$

where $j = 3, 4$ and $w_1 = 0, w_2 = 1$. Finally we remove the factor of $1/v_2$ from the right hand-side of the two equations and obtain the reduced equations. Note that the reduced equations are orbit equivalent to the original ones, but the absolute velocity is not preserved by the transformation as we removed the factor $1/v_2$.

The reduced system of two equations in complex variables is given by

$$\begin{aligned} \dot{w}_3 &= \frac{w_3 - 1}{|w_3 - 1|} + \frac{w_4}{|w_4|} - w_3 \left(1 + \frac{w_4}{|w_4|} \right) \\ \dot{w}_4 &= \frac{w_4 - w_3}{|w_4 - w_3|} + \frac{w_4}{|w_4|} - w_4 \left(1 + \frac{w_4}{|w_4|} \right). \end{aligned} \tag{3}$$

The degenerate bow-tie configuration corresponds to the fixed point $w_3 = 0, w_4 = 1$ while the square configurations correspond to the fixed points $w_3 = 1 \pm i, w_4 = 0 \pm i$. In the next section, we will study local dynamics in the vicinities of these configurations.

3.1. Linear analysis near bow-tie.

The Jacobian evaluated at the bow-tie configuration is given by

$$\mathbf{J} = \begin{bmatrix} -2 & 0 & 0 & 0 \\ 0 & -2 & 0 & 0 \\ 0 & 0 & -1 & 1 \\ 0 & 0 & -1 & -1 \end{bmatrix}.$$

Its spectrum consists of the eigenvalues

$$\text{spec}(\mathbf{J}) = \{-2, -2, -1 - i, -1 + i\}$$

with the eigenvectors

$$\mathbf{v}_1 = \begin{bmatrix} 0 \\ 1 \\ 0 \\ 0 \end{bmatrix}, \quad \mathbf{v}_2 = \begin{bmatrix} 1 \\ 0 \\ 0 \\ 0 \end{bmatrix}, \quad \mathbf{v}_3 = \begin{bmatrix} 0 \\ 0 \\ -i \\ 1 \end{bmatrix}, \quad \mathbf{v}_4 = \begin{bmatrix} 0 \\ 0 \\ i \\ 1 \end{bmatrix}.$$

Since all the real parts of the eigenvalues are negative, the bow-tie configuration is linearly asymptotically stable.

3.2. Linear analysis near square.

Fixing the orientation of the configuration one can easily distinguish between two different square configurations. Without any loss of generality we will consider the configuration corresponding to the point $w_3 = 1 + i$, $w_4 = i$. In order to shift the fixed point to the origin we will use four real variables x_1, x_2, y_1, y_2 defined as follows

$$w_3 = (1 + x_1) + i(1 + y_1)$$

$$w_4 = x_2 + i(1 + y_2).$$

As an example, we show here the equation for $x_1 = \mathcal{R}e(w_3) - 1$

$$\begin{aligned} \dot{x}_1 = & \frac{x_1}{\sqrt{x_1^2 + (y_1 + 1)^2}} - \frac{x_1 x_2}{\sqrt{x_2^2 + (y_2 + 1)^2}} - x_1 + \frac{y_1}{\sqrt{x_2^2 + (y_2 + 1)^2}} + \\ & \frac{y_1 y_2}{\sqrt{x_2^2 + (y_2 + 1)^2}} + \frac{y_2}{\sqrt{x_2^2 + (y_2 + 1)^2}} + \frac{1}{\sqrt{x_2^2 + (y_2 + 1)^2}} - 1. \end{aligned}$$

The other equations for x_2, y_1, y_2 can be easily generated by Mathematica notebook presented in the appendix.

Next, we compute the Jacobian of the system of differential equations where we ordered the variables as x_1, x_2, y_1, y_2 .

The matrix of partial derivatives, evaluated at $x_1 = x_2 = y_1 = y_2 = 0$, is given by

$$\mathbf{J} = \begin{bmatrix} 0 & 0 & 1 & 0 \\ 0 & 0 & 0 & 1 \\ -1 & -1 & -1 & 0 \\ 0 & -2 & -1 & 0 \end{bmatrix}$$

with eigenvalues

$$\text{spec}(\mathbf{J}) = \left\{ \frac{1}{2}(-1 + i\sqrt{7}), \frac{1}{2}(-1 - i\sqrt{7}), i, -i \right\}$$

and corresponding eigenvectors

$$\begin{aligned} \mathbf{v}_1 &= \begin{bmatrix} \frac{1}{4}(-i\sqrt{7} - 1) \\ \frac{1}{4}(-i\sqrt{7} - 1) \\ 1 \\ 1 \end{bmatrix}, & \mathbf{v}_3 &= \begin{bmatrix} 1 \\ -i \\ i \\ 1 \end{bmatrix}, \\ \mathbf{v}_2 &= \begin{bmatrix} \frac{1}{4}(i\sqrt{7} - 1) \\ \frac{1}{4}(i\sqrt{7} - 1) \\ 1 \\ 1 \end{bmatrix}, & \mathbf{v}_4 &= \begin{bmatrix} 1 \\ i \\ -i \\ 1 \end{bmatrix}. \end{aligned} \tag{4}$$

Vectors \mathbf{v}_1 and \mathbf{v}_2 correspond to parallelogram configurations. One can see that the real parts of the eigenvalues corresponding to these vectors are negative and so the square configuration is locally attracting in the direction of parallelograms. However, eigenvalues corresponding to the vectors $\mathbf{v}_3, \mathbf{v}_4$ have zero real parts. Therefore, the square configuration is neutrally stable in linear approximation. To determine nonlinear stability, we will need to investigate higher order terms. We will do so in section 5.

3.3. Degenerate cyclic configuration

The degenerate cyclic configurations form an invariant subset. None of these configurations correspond to a fixed point in the reduced system (3). Therefore, we do not determine linear stability. On the other hand, this invariant subset is unstable in the following sense: any nearly degenerate parallelogram arbitrarily close to degenerate cyclic configuration subset will converge to a square configuration, see the next section.

However, if one considers another special perturbation: one of the agents is slightly off the line, then the argument from Proposition 1 implies immediate loss of convexity.

4. Plane of parallelograms.

As it follows from the above discussion, the space of parallelograms is an eigenspace for the linear part of the cyclic evasion system near the square. Actually, one has a stronger statement

Lemma 1. *Space of parallelograms is invariant under the cyclic evasion evolution.*

Proof. In order to show this we will again use the coordinate system (2), see Figure 3. Since for the parallelogram one has

$$\ell_1 = \ell_3, \quad \ell_2 = \ell_4, \quad \alpha_1 = \alpha_3 = \pi - \alpha_2 = \pi - \alpha_4 \tag{5}$$

system (2) reduces to

$$\dot{\ell}_1 = 1 + \cos(\alpha_1), \quad \dot{\ell}_2 = 1 - \cos(\alpha_1), \quad \text{and} \quad \dot{\alpha}_1 = \frac{1}{\ell_1} - \frac{1}{\ell_2},$$

from where it follows that $\dot{\ell}_1 = \dot{\ell}_3$ and $\dot{\ell}_2 = \dot{\ell}_4$. Thus, lengths of the opposite sides remain equal during the evolution. Therefore, the evolving configuration remains in the parallelogram plane forever. \square

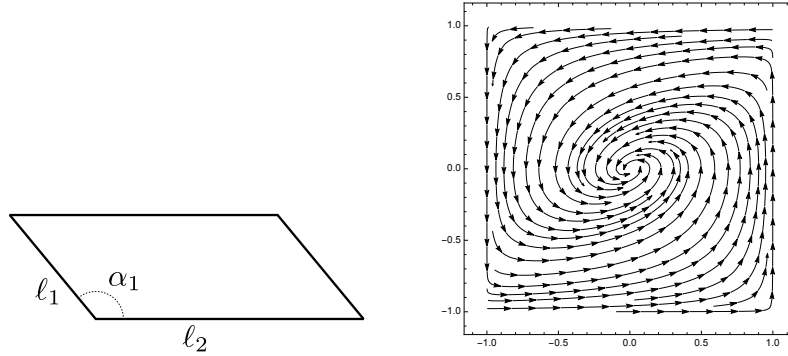


Figure 3. Left: Parallelogram configuration is completely determined by the angle α_1 and the aspect-ratio ℓ_1/ℓ_2 . Right: Square configuration is the attractor in the plane of parallelograms. Vector field for the evasion in (x, s) coordinates is presented.

To study the space of parallelograms, we use a change of coordinates that has been introduced in [7].

$$\begin{cases} s = \frac{\ell_1 - \ell_2}{\ell_1 + \ell_2} \\ x = \cos(\varphi_1) \end{cases} \quad (6)$$

In these variables, the space of parallelograms is parametrized by the open set $(-1, 1) \times (-1, 1) \subset \mathbb{R}^2$. Applying also the logarithmic change of time $\tau = -\log(-2t)$ the system (1) reduces to the form

$$\begin{cases} x' = -4s(1 - x^2)/(1 - s^2) \\ s' = 2(x - s), \end{cases} \quad (7)$$

where prime corresponds to the differentiation with respect to τ , see Figure 3.

It turns out the dynamics in the parallelogram plane is especially simple

Theorem 1. *Square configuration is the global attractor in the plane of parallelogram configurations.*

Proof. Let

$$F(x, s) = -\ln((1 - x^2)(1 - s^2)^2) \quad (8)$$

be a candidate for a Lyapunov function. It is easy to see that for all $(x, s) \in (-1, 1) \times (-1, 1)$, we have $(1 - x^2)(1 - s^2)^2 < 1$ so that $F(x, s)$ is everywhere nonnegative

on the phase space and the only solution for $F(x, s) = 0$ is the origin. Next we have to check that the derivative of $F(x, s)$ along the solutions of the system (7) is negative. Expressing $\frac{d}{dt}F = \nabla F \cdot (x', s')$ and substituting the corresponding expressions for x' and s' we get

$$F' = -\frac{-2x}{1-x^2} \cdot \frac{-4s(1-x^2)}{1-s^2} - \frac{-4s}{1-s^2} \cdot 2(x-s) = -8\frac{s^2}{1-s^2}.$$

The latter expression is negative everywhere whenever $s \neq 0$. Since for all points in the set $\mathcal{S} = \{(x, s) \mid s = 0\}$ only the origin remains in \mathcal{S} one can apply a variant of Lyapunov theorem, called Barbasin-Krasovskii theorem [4] that implies asymptotic stability of the point $(0, 0)$. \square

Remark. Function $F(x, s)$ has a nice geometric interpretation. From (7) it follows that $(1-s^2) = \frac{4\ell_1\ell_2}{(\ell_1+\ell_2)^2}$ and $1-x^2 = \sin^2 \alpha_1$. Thus $F(x, s)$ is proportional to the logarithm of the ratio between the area of the parallelogram and the square of its perimeter.

5. Nonlinear analysis of the dynamics near the square configuration.

According to the above analysis, the square configuration is only neutrally stable in linear approximation. To decide nonlinear stability we need to consider higher order terms in the equations. We use the standard combination of central manifold reduction with normal form analysis to arrive at the following

Theorem 2. *The square configuration is unstable in the sense of Lyapunov.*

To prove this theorem we use the algorithm developed in [10]. That is done with the aid of Mathematica software and the details of the calculations can be found in the appendix. Here, we give an outline of the approach.

Since there are two complex conjugate pairs of eigenvalues: $\pm i, \frac{1}{2}(-1 \pm \sqrt{7})$, by using eigenbasis, we can represent equations as a pair of ODEs in the complex plane

$$\begin{cases} \dot{\zeta}_1 = i\zeta_1 + f(\zeta_1, \bar{\zeta}_1, \zeta_2, \bar{\zeta}_2) \\ \dot{\zeta}_2 = \frac{1}{2}(-1 + i\sqrt{7})\zeta_2 + g(\zeta_1, \bar{\zeta}_1, \zeta_2, \bar{\zeta}_2). \end{cases} \quad (9)$$

According to the center manifold theorem, see *e.g.* [10], there exists two dimensional center manifold tangent to the two-dimensional subspace $\{\zeta_1, \bar{\zeta}_1\}$. The manifold is smooth and can be represented by power series:

$$\zeta_2 = a_{20}\zeta_1^2 + a_{11}\zeta_1\bar{\zeta}_1 + a_{02}\bar{\zeta}_1^2 + \dots \quad (10)$$

The coefficients of the expansion can be computed by the method of undetermined coefficients using the invariance property of the central manifold.

Substituting the expressions for $\zeta_2, \bar{\zeta}_2$ in (9), one obtains reduced equations for the dynamics on the central manifold

$$\dot{\zeta}_1 = i\zeta_1 + b_{20}\zeta_1^2 + b_{11}\zeta_1\bar{\zeta}_1 + b_{02}\bar{\zeta}_1^2 + \dots$$

Next, one applies normal form theory to eliminate non-resonant terms in the equation by applying smooth near-identical transformations, see *e.g.* [3]).

Recall that in a system of ODEs

$$\frac{d}{dt}\zeta = f(\zeta),$$

where $\zeta = (\zeta_1, \zeta_2, \dots, \zeta_s, \dots, \zeta_k)$ the monomial $\zeta_1^{m_1}\zeta_2^{m_2}\dots\zeta_k^{m_k}$ in the equation for ζ_s is resonant if

$$m_1\lambda_1 + m_2\lambda_2 + \dots + m_k\lambda_k = \lambda_s.$$

Resonant monomials cannot be eliminated by near identical transformations and they are essential for the dynamics.

In our case, the resonance condition takes the form

$$m_1i + m_2(-i) = i,$$

which implies that the only resonant term at order 3 or lower is $\zeta_1^2\bar{\zeta}_1$.

Therefore, our system can be transformed to the form

$$\dot{u} = iu + \sigma u^2\bar{u} + O(|u|^4),$$

where σ is the coefficient that decides stability or instability and $u = \zeta_1 + O(|\zeta_1|^2)$.

Computing σ is a straightforward but rather tedious procedure. The main complication is that when eliminating quadratic terms, the cubic terms are affected. Thus, one has to keep track of all transformations. We present the calculations in Mathematica notebook in the appendix. Our main conclusion is that $\mathcal{Re}(\sigma) = 0.06250 > 0$, which implies that square configuration is Lyapunov unstable. To independently verify this calculation, we also performed numerical simulations by starting with a small deformation of the square and letting the quadrilateral evolve in the equations obtained in Mathematica notebook (four ODEs for x_1, y_1, x_2, y_2).

One of the results is presented in Figure 4. The horizontal coordinate is time and the vertical coordinate represents the “distance” from the plane of parallelograms

$$d = \text{distance} = \sqrt{(x_1 - x_2)^2 + (y_1 - y_2)^2}.$$

We expect, based on the analysis, that $d(t)$ approximately satisfies the equation

$$\dot{d} = 0.0625 \cdot d^3.$$

Solving the equation, we obtain

$$\frac{1}{d^2(0)} - \frac{1}{d^2(1000)} = 2 \cdot 0.0625 \cdot 1000 = 125.$$

We observe from the Figure that $d(0) \approx 0.08$ and $d(1000) \approx 0.16$ and so the left hand-side of the equation approximately equals to 117.19 which is a reasonable agreement.

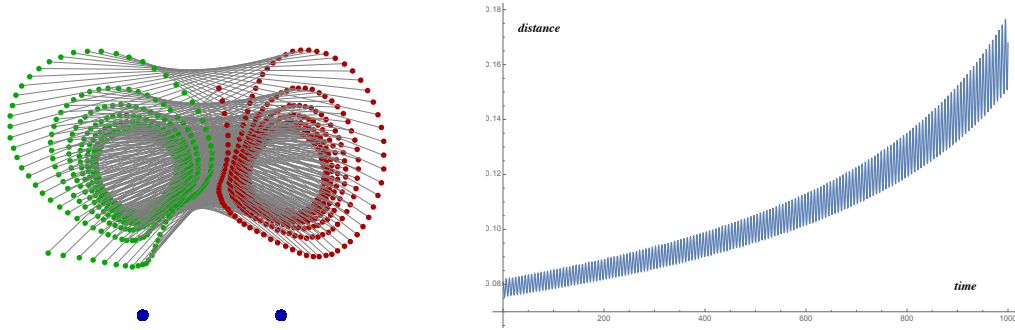


Figure 4. Nonlinear instability near the square configuration. Left: The perturbed square configuration oscillates around the square while the magnitude of oscillations is growing. The blue dots represent vertices $(0, 0)$ and $(1, 0)$. The red one is w_3 and the green one is w_4 . Right: Distance variable $d = \sqrt{(x_1 - x_2)^2 + (y_1 - y_2)^2}$ corresponds to the deviation from parallelogram.

6. Conclusions

We investigated the dynamics and stability of stationary configurations of the four agents evasion problem. Up to the translation, rotation, and scaling, there are only two stationary configurations: degenerate bow-tie which is locally asymptotically stable and square which is unstable. There is also a two-dimensional invariant set of parallelograms where all configurations asymptotically converge to the square.

Multiple simulations seem to suggest that a randomly drawn configuration converges to the degenerate bow-tie, see Figure 5. We know, however, that parallelograms do not converge to the bow-tie but rather converge to the square. Motivated by these observations, we state the hypothesis about global behavior.

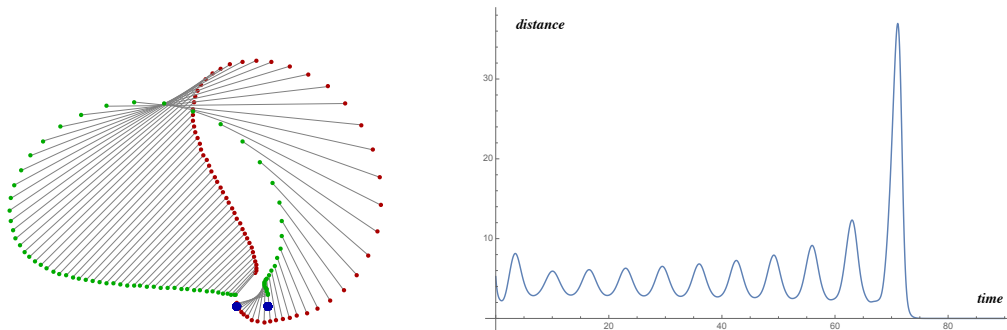


Figure 5. Convergence of a quadrilateral to degenerate bow-tie. Left: After the magnitude of the oscillation reaches the critical level, the configuration became trapped by the attraction region of the bow-tie configuration. Right: Distance variable $d = \sqrt{(x_1 + 1)^2 + (x_2 - 1)^2 + (y_1 + 1)^2 + (y_2 + 1)^2}$ corresponds to the distance from bow-tie.

Hypothesis: *If four agents are not in the vertices of parallelogram and do not belong*

to the same line then they converge to the degenerate bow-tie configuration.

References

- [1] M. Arnold, Yu. Baryshnikov, and D. Liberzon. Cyclic pursuit without coordinates: Convergence to regular polygon formations. In *53rd IEEE Conference on Decision and Control*, pages 6191–6196. IEEE, 2014.
- [2] M. Arnold and V. Zharnitsky. Cyclic evasion in the three bug problem. *The American Mathematical Monthly*, 122(4):377–380, 2015.
- [3] V.I. Arnold. *Geometrical Methods in the Theory of Ordinary Differential Equations*, volume 250. Springer-Verlag, 1988.
- [4] E. A. Barbasin and N. N. Krasovskii. On stability of motion in the large. *Doklady Akad. Nauk SSSR (N.S.)*, 86:453–456, 1952.
- [5] Yu. Baryshnikov and V. Zharnitsky. Sub-Riemannian geometry and periodic orbits in classical billiards. *Math. Res. Lett.*, 13(4):587–598, 2006.
- [6] F. Behroozi and R. Gagnon. Perimeter expansion in the n-bug system and its relationship to stability. *Journal of Mathematical Physics*, 22(4):656–662, 1981.
- [7] S.J. Chapman, J. Lottes, and L.N. Trefethen. Four bugs on a rectangle. *Proceedings of the Royal Society A*, 467(2127):881–896, 2011.
- [8] K. S. Galloway, E. W. Justh, and P. S. Krishnaprasad. Symmetry and reduction in collectives: cyclic pursuit strategies. *Proceedings of the Royal Society of London A: Mathematical, Physical and Engineering Sciences*, 469(2158), 2013.
- [9] D. Gekhtman. Cyclic pursuit on compact manifolds. *arxiv 1602.03259*, 2016.
- [10] Yuri A. Kuznetsov. *Elements of applied bifurcation theory*, volume 112 of *Applied Mathematical Sciences*. Springer-Verlag, New York, second edition, 1998.
- [11] Paul J. Nahin. *Chases and Escapes: The Mathematics of Pursuit and Evasion*. Princeton University Press, 2007.
- [12] T.J. Richardson. Stable polygons of cyclic pursuit. *Annals of Math. and Art. Intel.*, 31(1-4):147–172, 2001.
- [13] J. Yu, S.M. LaValle, and D. Liberzon. Rendezvous without coordinates. *47th IEEE Conference CDC2008*, pages 1803–1808, 2008.

Appendix A. Mathematica code.

Introduce vector fields. Compute Jacobian = A. Eigenvalues/eigenvectors.

$$\begin{aligned}
 w_1[\{x_1, x_2, y_1, y_2\}] &= (x_1 + 1) + i(y_1 + 1); \\
 w_2[\{x_1, x_2, y_1, y_2\}] &= x_2 + i(y_2 + 1); \\
 F_1[\{x_1, x_2, y_1, y_2\}] &= (w_1[\{x_1, x_2, y_1, y_2\}] - 1)/\text{Abs}[w_1[\{x_1, x_2, y_1, y_2\}] - 1] - \\
 &\quad w_1[\{x_1, x_2, y_1, y_2\}] + w_2[\{x_1, x_2, y_1, y_2\}]/\text{Abs}[w_2[\{x_1, x_2, y_1, y_2\}]] - \\
 &\quad w_1[\{x_1, x_2, y_1, y_2\}]w_2[\{x_1, x_2, y_1, y_2\}]\text{Abs}[w_2[\{x_1, x_2, y_1, y_2\}]]; \\
 F_2[\{x_1, x_2, y_1, y_2\}] &= (w_2[\{x_1, x_2, y_1, y_2\}] - w_1[\{x_1, x_2, y_1, y_2\}])/ \\
 &\quad \text{Abs}[w_2[\{x_1, x_2, y_1, y_2\}] - w_1[\{x_1, x_2, y_1, y_2\}]] - \\
 &\quad w_2[\{x_1, x_2, y_1, y_2\}] + w_1[\{x_1, x_2, y_1, y_2\}]/\text{Abs}[w_1[\{x_1, x_2, y_1, y_2\}]] - \\
 &\quad w_2[\{x_1, x_2, y_1, y_2\}]w_1[\{x_1, x_2, y_1, y_2\}]/\text{Abs}[w_1[\{x_1, x_2, y_1, y_2\}]]; \\
 F_{1,x}[\{x_1, x_2, y_1, y_2\}] &= \text{ComplexExpand}[\text{Re}[F_1[\{x_1, x_2, y_1, y_2\}]]]; \\
 F_{2,x}[\{x_1, x_2, y_1, y_2\}] &= \text{ComplexExpand}[\text{Re}[F_2[\{x_1, x_2, y_1, y_2\}]]];
 \end{aligned}$$

```

F1,y[{x1, x2, y1, y2}] = ComplexExpand[Im[F1[{x1, x2, y1, y2}]]];
F2,y[{x1, x2, y1, y2}] = ComplexExpand[Im[F2[{x1, x2, y1, y2}]]];
A = Evaluate[D[{F1,x[{x1, x2, y1, y2}], F2,x[{x1, x2, y1, y2}], F1,y[{x1, x2, y1, y2}], F2,y[{x1, x2, y1, y2}]}],
  {{x1, x2, y1, y2}}]/.{x1 -> 0, x2 -> 0, y1 -> 0, y2 -> 0};
spec = Eigenvalues[A]; //echo
vec = Eigenvectors[A]; //echo

```

$$\begin{aligned}
spec &= \left\{ \frac{1}{2}(-1 + i\sqrt{7}), \frac{1}{2}(-1 - i\sqrt{7}), i, -i \right\} \\
vec &= \left\{ \left\{ \frac{1}{4}(-1 - i\sqrt{7}), \frac{1}{4}(-1 - i\sqrt{7}), 1, 1 \right\}, \right. \\
&\quad \left. \left\{ \frac{1}{4}(-1 + i\sqrt{7}), \frac{1}{4}(-1 + i\sqrt{7}), 1, 1 \right\}, \{1, -i, i, 1\}, \{1, i, -i, 1\} \right\}
\end{aligned}$$

Algorithm to compute Lyapunov coefficient. From the book by Kuznetsov [10], pages 492-494, Steps 0-6.

First find eigenvector corresponding to imaginary eigenvalue, normalize it, and find its real and imaginary parts.

```

q = Normalize[vec[[3]]];
{qr = Re[q], qi = Im[q]}; //echo

```

$$\begin{aligned}
qr &= \left\{ \frac{1}{2}, 0, 0, \frac{1}{2} \right\} \\
qi &= \left\{ 0, -\frac{1}{2}, \frac{1}{2}, 0 \right\}
\end{aligned}$$

Next find adjoint eigenvector p, normalize it, and find its real and imaginary parts.

```

ATR = Transpose[A];
spectr = Eigenvalues[ATR]; //echo
vectr = Eigenvectors[ATR];
p = vectr[[4]]/(1 + I); //echo
pr = Re[p]; //echo
pi = Im[p]; //echo

```

$$\begin{aligned}
spectr &= \left\{ \frac{1}{2}(-1 + i\sqrt{7}), \frac{1}{2}(-1 - i\sqrt{7}), i, -i \right\} \\
p &= \left\{ \frac{1}{2} + \frac{i}{2}, -\frac{1}{2} - \frac{i}{2}, -\frac{1}{2} + \frac{i}{2}, \frac{1}{2} - \frac{i}{2} \right\} \\
pr &= \left\{ \frac{1}{2}, -\frac{1}{2}, -\frac{1}{2}, \frac{1}{2} \right\} \\
pi &= \left\{ \frac{1}{2}, -\frac{1}{2}, \frac{1}{2}, -\frac{1}{2} \right\}
\end{aligned}$$

Find directional derivatives of order 2 along the direction qr

```

a = Evaluate[D[{F1,x[tqr], F2,x[tqr], F1,y[tqr], F2,y[tqr]}], {t, 2}]/.{t -> 0}; //echo

```

$$a = \left\{ 0, \frac{1}{4}, -\frac{1}{4}, -\frac{1}{2} \right\}$$

Find directional derivatives of order 2 along q_i

```
b = Evaluate[D[{F1,x[tqi], F2,x[tqi], F1,y[tqi], F2,y[tqi]}, {t, 2}]]/.{t -> 0}; //echo
```

$$b = \left\{ -\frac{1}{4}, -\frac{1}{2}, \frac{1}{2}, \frac{1}{4} \right\}$$

Now find directional derivatives along sum and difference of $qr + qi$ and $qr - qi$

```
c = 0.25 * Evaluate[D[{F1,x[t(qr + qi)] - F1,x[t(qr - qi)], F2,x[t(qr + qi)] - F2,x[t(qr - qi)],
F1,y[t(qr + qi)] - F1,y[t(qr - qi)], F2,y[t(qr + qi)] - F2,y[t(qr - qi)]}, {t, 2}]]/.
{t -> 0}; //echo
```

$$c = \{0., 0., -0.25, 0.\}$$

Find solutions of two linear systems, one is real r , the other solution is complex $s = sR + i sI$.

```
r = LinearSolve[A, a + b]; //echo
```

```
s = LinearSolve[2 * I * IdentityMatrix[4], a - b + I * 2 * c];
```

```
sR = Re[s]; //echo
```

```
sI = Im[s]; //echo
```

$$r = \left\{ -\frac{1}{4}, \frac{1}{4}, -\frac{1}{4}, -\frac{1}{4} \right\}$$

$$sR = \{0., 0., -0.25, 0.\}$$

$$sI = \{-0.125, -0.375, 0.375, 0.375\}$$

Now compute σ_1 and σ_2 .

```
sgm1 = 0.25 * pr.(Evaluate[D[{F1,x[t(qr + r)] - F1,x[t(qr - r)],
F2,x[t(qr + r)] - F2,x[t(qr - r)], F1,y[t(qr + r)] - F1,y[t(qr - r)],
F2,y[t(qr + r)] - F2,y[t(qr - r)]}, {t, 2}]]/.{t -> 0}); //echo
```

```
sgm2 = 0.25 * pi.(Evaluate[D[{F1,x[t(qi + r)] - F1,x[t(qi - r)],
F2,x[t(qi + r)] - F2,x[t(qi - r)], F1,y[t(qi + r)] - F1,y[t(qi - r)],
F2,y[t(qi + r)] - F2,y[t(qi - r)]}, {t, 2}]]/.{t -> 0}); //echo
```

```
sigma = sgm1 + sgm2; //echo
```

$$sgm1 = 0.0625$$

$$sgm2 = -0.0625$$

$$\sigma = 0.$$

Step 5: Computing deltas

```

 $\delta_1 = \text{pr.}(0.25 * \text{Evaluate}[\text{D}[\{\text{F}_{1,x}[\text{t}(\text{qr} + \text{sR})] - \text{F}_{1,x}[\text{t}(\text{qr} - \text{sR})], \text{F}_{2,x}[\text{t}(\text{qr} + \text{sR})] - \text{F}_{2,x}[\text{t}(\text{qr} - \text{sR})],$ 
 $\text{F}_{1,y}[\text{t}(\text{qr} + \text{sR})] - \text{F}_{1,y}[\text{t}(\text{qr} - \text{sR})], \text{F}_{2,y}[\text{t}(\text{qr} + \text{sR})] - \text{F}_{2,y}[\text{t}(\text{qr} - \text{sR})]\}, \{\text{t}, 2\}]/.$ 
 $\{\text{t} \rightarrow 0\}); //\text{echo}$ 

```

```

 $\delta_2 = \text{pr.}(0.25 * \text{Evaluate}[\text{D}[\{\text{F}_{1,x}[\text{t}(\text{qi} + \text{sI})] - \text{F}_{1,x}[\text{t}(\text{qi} - \text{sI})], \text{F}_{2,x}[\text{t}(\text{qi} + \text{sI})] - \text{F}_{2,x}[\text{t}(\text{qi} - \text{sI})],$ 
 $\text{F}_{1,y}[\text{t}(\text{qi} + \text{sI})] - \text{F}_{1,y}[\text{t}(\text{qi} - \text{sI})], \text{F}_{2,y}[\text{t}(\text{qi} + \text{sI})] - \text{F}_{2,y}[\text{t}(\text{qi} - \text{sI})]\}, \{\text{t}, 2\}]/.$ 
 $\{\text{t} \rightarrow 0\}); //\text{echo}$ 

```

```

 $\delta_3 = \text{pi.}(0.25 * \text{Evaluate}[\text{D}[\{\text{F}_{1,x}[\text{t}(\text{qr} + \text{sI})] - \text{F}_{1,x}[\text{t}(\text{qr} - \text{sI})], \text{F}_{2,x}[\text{t}(\text{qr} + \text{sI})] - \text{F}_{2,x}[\text{t}(\text{qr} - \text{sI})],$ 
 $\text{F}_{1,y}[\text{t}(\text{qr} + \text{sI})] - \text{F}_{1,y}[\text{t}(\text{qr} - \text{sI})], \text{F}_{2,y}[\text{t}(\text{qr} + \text{sI})] - \text{F}_{2,y}[\text{t}(\text{qr} - \text{sI})]\}, \{\text{t}, 2\}]/.$ 
 $\{\text{t} \rightarrow 0\}); //\text{echo}$ 

```

```

 $\delta_4 = \text{pi.}(0.25 * \text{Evaluate}[\text{D}[\{\text{F}_{1,x}[\text{t}(\text{qi} + \text{sR})] - \text{F}_{1,x}[\text{t}(\text{qi} - \text{sR})], \text{F}_{2,x}[\text{t}(\text{qi} + \text{sR})] - \text{F}_{2,x}[\text{t}(\text{qi} - \text{sR})],$ 
 $\text{F}_{1,y}[\text{t}(\text{qi} + \text{sR})] - \text{F}_{1,y}[\text{t}(\text{qi} - \text{sR})], \text{F}_{2,y}[\text{t}(\text{qi} + \text{sR})] - \text{F}_{2,y}[\text{t}(\text{qi} - \text{sR})]\}, \{\text{t}, 2\}]/.$ 
 $\{\text{t} \rightarrow 0\}); //\text{echo}$ 

```

```

 $\delta = \delta_1 + \delta_2 + \delta_3 - \delta_4; //\text{echo}$ 

```

$$\delta_1 = -0.0625$$

$$\delta_2 = -0.03125$$

$$\delta_3 = -0.09375$$

$$\delta_4 = 0.0625$$

$$\delta = -0.25$$

Step 6: Compute 3rd derivatives and gammas.

```

 $\gamma_1 = \text{pr.}(\text{Evaluate}[\text{D}[\{\text{F}_{1,x}[\text{tqr}], \text{F}_{2,x}[\text{tqr}], \text{F}_{1,y}[\text{tqr}], \text{F}_{2,y}[\text{tqr}]\}, \{\text{t}, 3\}]/.\{\text{t} \rightarrow 0\}); //\text{echo}$ 

```

```

 $\gamma_2 = \text{pi.}(\text{Evaluate}[\text{D}[\{\text{F}_{1,x}[\text{tqi}], \text{F}_{2,x}[\text{tqi}], \text{F}_{1,y}[\text{tqi}], \text{F}_{2,y}[\text{tqi}]\}, \{\text{t}, 3\}]/.\{\text{t} \rightarrow 0\}); //\text{echo}$ 

```

```

 $\gamma_3 = (\text{Evaluate}[\text{D}[\{\text{F}_{1,x}[\text{t}(\text{qr} + \text{qi})], \text{F}_{2,x}[\text{t}(\text{qr} + \text{qi})], \text{F}_{1,y}[\text{t}(\text{qr} + \text{qi})], \text{F}_{2,y}[\text{t}(\text{qr} + \text{qi})]\}, \{\text{t}, 3\}]]$ 
 $/. \{\text{t} \rightarrow 0\}).(\text{pr} + \text{pi}); //\text{echo}$ 

```

```

 $\gamma_4 = (\text{Evaluate}[\text{D}[\{\text{F}_{1,x}[\text{t}(\text{qr} - \text{qi})], \text{F}_{2,x}[\text{t}(\text{qr} - \text{qi})], \text{F}_{1,y}[\text{t}(\text{qr} - \text{qi})], \text{F}_{2,y}[\text{t}(\text{qr} - \text{qi})]\}, \{\text{t}, 3\}]]$ 
 $/. \{\text{t} \rightarrow 0\}).(\text{pr} - \text{pi}); //\text{echo}$ 

```

```

 $\gamma = (\gamma_1 + \gamma_2) * 2/3 + (\gamma_3 + \gamma_4)/6; //\text{echo}$ 

```

```

 $\text{Lyapunov} = (\gamma - 2 * \text{sigma} + \delta)/2; //\text{echo}$ 

```

$$\gamma_1 = \frac{3}{8}$$

$$\gamma_2 = \frac{3}{8}$$

$$\gamma_3 = -\frac{3}{4}$$

$$\gamma_4 = 0$$

$$\gamma = \frac{3}{8}$$

$$\text{Lyapunov} = 0.0625$$